Heliyon

ELSEVIER

Received:
3 June 2018
Revised:
28 September 2018
Accepted:
6 December 2018

Cite as: Qinfang Deng, Boxiong Xie, Leilei Wu, Xianxiu Ji, Chao Li, Li Feng, Qiyu Fang, Yuchen Bao, Jialu Li, Shengnan Jin, Chunming Ding, Yixue Li, Songwen Zhou. Competitive evolution of NSCLC tumor clones and the drug resistance mechanism of first-generation EGFR-TKIs in Chinese NSCLC patients. Heliyon 4 (2018) e01031. doi: 10.1016/j.heliyon.2018.e01031

Competitive evolution of NSCLC tumor clones and the drug resistance mechanism of first-generation EGFR-TKIs in Chinese NSCLC patients

Qinfang Deng [a,1], Boxiong Xie [b,1], Leilei Wu [c,1], Xianxiu Ji [a,1], Chao Li [f], Li Feng [e], Qiyu Fang [a], Yuchen Bao [a], Jialu Li [g], Shengnan Jin [g], Chunming Ding [g], Yixue Li [c,d,e,*], Songwen Zhou [a,]**

[a] *Department of Oncology, Shanghai Pulmonary Hospital, Tongji University School of Medicine, Shanghai, 200433, China*

[b] *Department of Thoracic, Shanghai Pulmonary Hospital, Tongji University School of Medicine, Shanghai, 200433, China*

[c] *School of Life Sciences and Biotechnology, Shanghai Jiao Tong University, Shanghai, 200240, China*

[d] *Bio-Med Big Data Center, CAS-MPG Partner Institute for Computational Biology, Shanghai Institute of Nutrition and Health, Shanghai Institutes for Biological Sciences, University of Chinese Academy of Sciences, Chinese Academy of Sciences, Shanghai, 200031, China*

[e] *CAS Key Laboratory for Computational Biology, CAS-MPG Partner Institute for Computational Biology, Shanghai Institute of Nutrition and Health, Shanghai Institute for Biological Sciences, University of Chinese Academy of Sciences, Chinese Academy of Sciences, Shanghai, 200031, China*

[f] *Smartquerier Biomedicine, Shanghai, 201203, China*

[g] *School of Laboratory Medicine and Life Sciences, Wenzhou Medical University, Wenzhou, Zhejiang, 325035, China*

[*] Corresponding author.

[**] Corresponding author.

E-mail addresses: yxli@sibs.ac.cn (Y. Li), songwenzhou2017@vip.126.com (S. Zhou).

[1] These authors contributed equally to this work.

Abstract

Purpose: Although many studies have reported on the resistance mechanism of first-generation EGFR TKIs (1st EGFR TKIs) treatment, large-scale dynamic ctDNA mutation analysis based on liquid biopsy for non-small cell lung cancer (NSCLC)

https://doi.org/10.1016/j.heliyon.2018.e01031

in the Chinese population is rare. Using in-depth integration and analysis of ctDNA genomic mutation data and clinical data at multiple time points during the treatment of 53 NSCLC patients, we described the resistance mechanisms of 1st EGFR TKIs treatment more comprehensively and dynamically. The resulting profile of the polyclonal competitive evolution of the tumor provides some new insights into the precise treatment of NSCLC.

Experimental design: A prospective study was conducted in patients with advanced NSCLC with acquired resistance to erlotinib, gefitinib or icotinib. By liquid biopsy, we detected mutations in 124 tumor-associated genes in the context of drug resistance. These 124 genes covered all tumor therapeutic targets and related biological pathways. During the entire course of treatment, the interval between two liquid biopsies was two months.

Results: Unlike the common mutations tested in tissue samples, our data showed a higher coverage of tumor heterogeneity (32.65%), more complex patterns of resistance and some new resistance mutation sites, such as EGFR p.V769M and KRAS p.A11V. The major resistance-associated mutations detected were still EGFR p.T790M (45.28%), other point mutations in *EGFR* (33.9%), and *KRAS* and *NRAS* mutations (15.09%). These mutation ratios might be considered as a preliminary summary of the characteristics of Chinese patients. In addition, starting from the two baseline mutations of the *EGFR* gene (19del vs. L858R), we first described the detailed mutation profile of the *EGFR* gene. Although there was no significant difference in the number of patients with EGFR p.19del and EGFR p.L858R baseline mutations (24% vs. 16%, $P = 0.15$), patients from the EGFR p.19del baseline group were much more likely to develop EGFR p.T790M resistance mutations (62.1% vs. 19.3%, $P = 0.007$). Through careful integration of gene mutation information and clinical phenotype information, an interesting phenomenon was found. Although the variant allele fraction (VAF) of the EGFR p.T790M mutation was significantly linearly correlated with that of the EGFR drug-sensitive mutation ($r = 0.68$, $P = 0.00025$), neither VAF was associated with the tumor volume at the advanced stage. It was shown that other tumor clones might contribute more to the resistance to 1st EGFR TKIs treatment than tumor clones carrying the EGFR p.T790M mutation when resistance developed. By further analysis, we found that, in some patients, when the primary tumor clones detected were those carrying EGFR−/− mutations (both types the EGFR p.19del/p.L858R and EGFR p.T790M mutation types were missing), most of them showed a poor prognosis and ineffective late treatment, indicating that EGFR−/− played a more important role than EGFR p.T790M in the process of NSCLC drug resistance in these patients. From the perspective of the clonal evolution of NSCLC tumor cells, these phenomena could be explained by the competitive evolution between different tumor clones. In addition, two new mutations, KRAS p.A11V and EGFR p.V769M, emerged significantly during drug resistance in NSCLC patients and had shown obvious competitive

https://doi.org/10.1016/j.heliyon.2018.e01031

clonal evolution characteristics. Combined with clear clinical drug resistance phenotypic information, we believed that these two new mutations might be related to new drug resistance mechanisms and deserve further study. We have also seen an interesting phenomenon. In some patients undergoing 1st EGFR TKIs treatment, the EGFR p.T790M mutation appeared, disappeared, and reappeared, and this spatial and temporal diversity of the EGFR p.T790M mutation was regulated by targeted drug and chemotherapy and was correlated with the individual tumor mutation profile.

Conclusions: The constitution and competitive evolution of the tumor clones have a decisive influence on treatment and can be regulated by targeted drugs and chemotherapy. Additionally, EGFR p.T790M spatial and temporal diversity during treatment warrants more attention, and this spatial and temporal diversity may be useful for the choice of treatment strategies for certain NSCLC patients. Through longitudinal cfDNA sample analysis, the resistance mechanism and dynamic clinical features of Chinese NSCLC patients are systematically established as reliable and meaningful to understand acquired resistance and make further personalized treatment decisions dynamically. Two new potential drug resistance-associated mutations in *EGFR* and *KRAS* have been found and are worthy of further study. Finally, our research shows that the evolutionary process of tumor cloning can be artificially regulated and intervened, possibly providing a new way to treat tumors.

Keyword: Oncology

1. Introduction

Targeted therapy represented by the 1st EGFR TKIs represents an important historical event in the history of non-small cell lung cancer (NSCLC) treatment and marks the advent of personalized therapy for the precise treatment of tumors. Epidermal growth factor receptor (*EGFR*) kinase inhibitors, such as gefitinib and erlotinib, have demonstrated efficacy in NSCLC patients with EGFR-sensitive mutations [1, 2]. Compared with chemotherapy, 1st EGFR-TKIs is well tolerated, can prolong patient progression-free survival (PFS) and can effectively improve the quality of life of patients [3, 4]. Despite the high efficacy, most patients acquire resistance to TKIs after 9–13 months of treatment [5]. In the Western population, resistance mechanisms and corresponding treatment strategies have been well studied [6, 7, 8, 9, 10, 11], but corresponding work is lacking for the Chinese population.

The main challenge for individualized treatment of cancer is tumor heterogeneity. Although the heterogeneity of NSCLC has been well studied [12, 13], the quantitative impact of tumor heterogeneity on treatment remains an interesting topic. For patients with advanced NSCLC, due to the limitations of traditional tissue biopsy

https://doi.org/10.1016/j.heliyon.2018.e01031

methods and deficiencies of previously used clinical mutation detection methods, we lack a clear and effective method to obtain more comprehensive somatic mutation information in NSCLC patients to show the multidrug resistance mechanism and characterize the detailed relationship between multidrug resistance mechanisms and the 1st EGFR-TKIs clinical response and PFS. There is also a lack of effective and quantitative methods to study the dynamic relationship between the mutation frequency (VAF) and changes in tumor volume to guide treatment. In this situation, precise treatment of NSCLC has not been completely resolved.

The analysis of circulating tumor DNA (ctDNA) based on next-generation sequencing (NGS) technology has many advantages over tumor tissue biopsy. First, unlike tissue samples, mutational information obtained from ctDNA is derived from almost all tumor subclones in tumor tissue. Second, by dynamically tracking patient prognosis information, it is easy to monitor the evolutionary status of tumor clones. Finally, the sampling process is minimally invasive [14]. Here, we used the high-sensitivity and high-specificity mutation detection method from ctDNA proposed by Aaron et al. [15] to study the mechanism of EGFR-TKI resistance. We dynamically monitored the ctDNA mutation spectrum in 53 Chinese patients with advanced NSCLC and integrated their complete clinical treatment information. Our research shows that the ctDNA mutation spectrum obtained from multiple follow-ups can enable studies of the dynamic changes in different tumor subclones and identify the factors that influence and regulate the evolution of tumor clones.

Our study found that the mutated profile of tumors after first-generation EGFR-TKI treatment obtained by liquid biopsy was consistent with the large change trend of the mutation profile obtained through tissue detection in the past. However, for the first time, we observed in depth the complex dynamic changes in the composition and proportion of tumor subclones in patients with NSCLC. It was found that this change was determined to some extent by the patient's baseline mutation profile and affected the treatment effect and prognosis. Furthermore, we discovered new possible resistance mutations that warrant further investigation. The methods, research ideas and results proposed in the current study provide new insights into the resistance mechanism of 1st EGFR TKIs therapy from the perspective of clonal evolution and provide practical clinical treatments for the targeted therapy of NSCLC patients.

2. Materials and methods

2.1. Patient enrollment and sample preparation

From May 2014 to July 2017, 53 patients with NSCLC at Shanghai Pulmonary Hospital were enrolled in this study approved by Medical Ethics Committee of Shanghai Pulmonary Hospital and provided informed consent. A follow-up information management system for lung cancer was used for standard follow-up. All patients had

https://doi.org/10.1016/j.heliyon.2018.e01031

EGFR drug-sensitive mutations and received 1st EGFR TKIs treatment when they entered the group and developed resistance. Baseline specimens with tumor content greater than 50% were collected from lung cancer tissues, pleural effusions, and tumor aspiration fluids. Peripheral blood samples from each patient were collected at the time of drug resistance. Among them, the blood cfDNA samples of 21 patients were collected every two months, followed by the performance of dynamic cfDNA series monitoring until the disease progressed. All blood samples were subjected to capture sequencing in real-time. The captured target gene panel was designed by Smartquerier Co., Ltd. and involved 124 tumor-associated genes (Supplementary Table 1). The sequencing instrument was from the Shanghai Academy of Sciences, and the platform used was Illumina HiSeq X10. The average sequencing depth was greater than 10000×.

2.2. Computed tomography and tumor volume assessment

The clinical staging of patients was performed using chest CT, whole-body bone scans, brain MRI, and abdominal ultrasound. Laboratory tests included serum tumor marker measurements. All patients who received 1st EGFR TKIs therapy were followed up for one month after the start of treatment and then every two months. A medical doctor who was blind to the initial CT report reviewed all CT scans. The 1st EGFR TKIs efficacy evaluation (Progressive Disease: PD; Stable Disease: SD; Partial Response: PR) was determined according to the RECIST 1.1 standard [16]. PD is defined as sum of the longest diameters (SLD) increased by at least 20% from the smallest value on study; PR is defined as at least a 30% decrease in the SLD of target lesions, taking as reference the baseline sum diameters; SD is defined as neither sufficient shrinkage to qualify for PR nor sufficient increase to qualify for PD. The tumor volume was determined from the CT scan of the tumor, the maximum tumor diameter was recorded as the length, the corresponding maximum vertical diameter was recorded as the width, and the tumor volume was calculated using the following expression: length*width*width/2 [17, 18].

2.3. Baseline mutation detection

Genomic DNA was extracted from baseline samples using the AmoyDx DNA/RNA kit. The somatic mutation test was performed using the AmoyDx® Assay Kit (detection resolution: 1%). The somatic mutations tested included 29 common *EGFR* mutations, 7 common *KRAS* mutations, and *ALK* fusions, *ROS1* fusions, and BRAF p.V600E.

2.4. DNA extraction

The patient's tumor samples and peripheral blood were collected in BCT (Streck) without cellular DNA contamination. Plasma was separated by centrifugation at

https://doi.org/10.1016/j.heliyon.2018.e01031

2,500×g for 10 minutes, transferred to a microfuge tube, and centrifuged at 16,000 ×g for 10 minutes to remove cell debris, and then peripheral blood leukocytes were obtained. Genomic DNA was isolated from the obtained peripheral blood leukocytes using the QIAamp DNA Blood Kit (Qiagen). Circulating free DNA was isolated from 3-5 mL of plasma using the QIAamp Circulating Nucleic Acid Kit.

2.5. Gene library preparation and sequencing

Indexed Illumina NGS libraries were prepared from plasma DNA and germline genomic DNA. For patient plasma DNA, 20−30ng of DNA was used for library construction without additional fragmentation. For germ cell genomic DNA, 200−1000ng of DNA was fragmented using the Covaris instrument and recommended fragment length setting of 200bp, and then library construction was performed. An NGS library was constructed using the KAPA library preparation kit (Kapa Biosystems). Agencourt AMPure XP beads (Beckman-Coulter) were used to purify the extracted DNA. A 100-fold mole excess of ligation Illumina TruSeq adaptors was used for ligation at 16 °C for 16 hours. By adding 40μL (0.8×) PEG buffer to enrich the ligated DNA fragments, and then single-step size selection of DNA fragments was performed. The ligated fragments were then amplified using 500nM of Illumina backbone oligonucleotides and 4−9 PCR cycles based on the input DNA mass.

The library concentration was assessed by Qubit and Qpcr. The fragment length was determined on a 2100 bioanalyzer using the DNA 1000 kit (Agilent). The library uses a customized NimbleGen SeqCap EZ Choice Library for hybridization selection. Eight and ten indexed Illumina libraries were included in single-capture hybridization. After hybridization selection, the captured DNA fragments were mixed with 50μL of KAPA HiFi Hot Start Ready Mix (1×) and 2μM of Illumina backbone oligonucleotides, and PCR was performed after 4 to 6 independent 12- to 14-cycle PCR, and the product was then pooled and subjected to the QIAquick PCR Purification Kit (Qiagen). Finally, 2 × 150 bp pair-end sequencing of the acquired multiple libraries was performed using Illumina HiSeq X10.

2.6. Analysis of sequencing results

The paired reads were aligned to the hg19 reference genome using the BWA (V0.7.15-r1140)-mem [19] command and were ranked and indexed using SAMtools (V1.3) [20]. QC uses a customized Python script to evaluate the various statistics collected, including comparison features, read quality, and panel capture efficiency. Based on IDES analysis flow [15], we developed virtual barcode based algorithm for variant calling. Briefly, our calling algorithm utilized a novel platform-independent virtual barcode (start + template length) strategy to cluster sequence reads into corresponding virtual consensuses that could eliminate random read-level errors,

https://doi.org/10.1016/j.heliyon.2018.e01031

followed by constructing distribution to polish stereotypical background artifacts. And three fine tuning filters applied to remove stochastic consensus level variants. Background noise filtering was performed using cfDNA data sets from 14 healthy people. For candidates, we selected a strict template number criterion (at least 4 templates) based on 'Poisson' distribution at 99% confidential level. AF values were calculated by following format: mutant read numbers/total reads (Supplementary Table 2). Detailed calling process referred to manuscript t (Wu et al; submitted). INDEL calling was performed using Vardict (V1.4.5) [21] and mutect2 [22], gene fusion was detected using FACTERA [23], CNV was detected using CNVkit [24], and the found mutation was annotated using ANNOVAR [25].

2.7. Mutation validation by droplet digital PCR

2.7.1. Circulating-free DNA extraction

Cell free DNA was isolated using Apostle MiniMaxTM High Efficiency cfDNA Isolation Kit (Standard Edition) according to the manufacturer's protocol. DNA was eluted in EB buffer (53 μl) and stored at −80 °C until use.

2.7.2. Droplet digital PCR workflow

PCR reactions, in 20 μl volume, consisted of 9 μl cfDNA, 0.3 μM of each primer, 0.1 μM of each probe, and 2× ddPCR Supermix (Bio-Rad). The mixture was loaded into sample wells of an eight-channel disposable droplet generator cartridge (Bio-Rad). An additional 70 μl of droplet generation oil (Bio-Rad) was loaded into the oil well for each channel. After droplet generation the cartridge was removed and manually transferred with a 200 μl pipet to a 96-well PCR plate. The plate was heat-sealed, placed on a thermocycler (Bio-Rad T100) with the following program: 95 °C 10 min, (94 °C 30 sec, 56/58/60*°C 1 min) × 45 cycles (2°C/sec ramp rate each step during the cycling), 98 °C 10 min, 10 °C forever. After PCR, the 96-well PCR plate was read on the QX-100 droplet reader (Bio-Rad). Analysis of the ddPCR data was performed with QuantaSoft analysis software (Bio-Rad) that accompanied the droplet reader.

2.7.3. Droplet digital PCR materials

Droplet digital PCR reagents were ordered from Bio-Rad. Primer/probe mix for TP53 c.A358T, TP53 c.G733T, EGFR c.T2240C were custom-made by TSINGKE Biological Technology. The allele-specific MGB probes are labeled with either VIC or FAM at the 5′ end. For TP53 c.A358T assay, primer sequences are: forward, 5′-GGCAACTGACCGTGCAAGT-3′, reverse, 5′-CGTCTGGGCTTCTTGCATTC-3′; probe sequences are: 5′-VIC- ACAGACTTGGCTGTCC-MGB-3′, 5′-FAM-A-CAGACTAGGCTGTC-MGB-3′. For TP53 c.G733T assay, primer sequences

https://doi.org/10.1016/j.heliyon.2018.e01031

are: forward, 5′-GAGTCTTCCAGTGTGATGATGGT-3′, reverse, 5′-TCCTAGGTTGGCTCTGACTGT-3′; probe sequences are: 5′-VIC-TCATGCCGCCCATG-MGB-3′, 5′-FAM-CGGTTCATGCAGC-MGB-3′. For EGFR c.T2240C assay, primer sequences are: forward, 5′- TCCCAGAAGGTGA-GAAAGTTAAAATT-3′, reverse, 5′-TGGCTTTCGGAGATGTTGCT-3′; probe sequences are: 5′-VIC- CTATCAAGGAATTAAGAG-MGB-3′, 5′-FAM-CTATCAAGGAATCAAG-MGB-3′. For TP53 c.A358T assay, the annealing temperature is 56 °C. For TP53 c.G733T assay, the annealing temperature is 58 °C. For EGFR c.T2240C assay, the annealing temperature is 60 °C. Validation result showed a good congruence in AF value between our calling result and ddPCR result (Supplementary Table 2).

2.8. Statistical analysis

2.8.1. PFS curve and Cox model construction

PFS time was calculated from the date of the 1st EGFR TKIs treatment to that of the advanced phase. The total survival time was calculated from the TKI treatment date to the end of the study. Patients who lost or survived after the end of the study were excluded. Kaplan-Meier estimates were used to generate progression-free survival curves and overall survival curves for different subpopulations—for example, EGFR p.19del vs. EGFR p.L858R and EGFR p.T790M positive vs. EGFR p.T790M negative. Differences between survival curves were analyzed using the log-rank test. In addition, the median survival time for different groups was calculated. A Cox proportional hazards regression model containing all measured covariates was constructed, and the hazard ratio (HR) was calculated to assess the importance of EGFR p.T790M and other covariates for progression-free survival.

2.8.2. Estimation of the tumor volume contribution by EGFR−/− subclones in EGFR p.T790M-positive patients

Of the 53 patients enrolled, 20 developed T790M with drug-responsive mutations, among whom only 12 patients had measurable tumor foci. To obtain reliable statistical estimates of the EGFR−/− tumor volume in patients with EGFR p.T790M mutations, we added another six patients with EGFR p.T790M mutation and corresponding drug-sensitive mutations who met the inclusion criteria at resistance. We assumed that the contribution to the size of the patient's tumor tissue came from two tumor subclones, EGFR−/− and EGFR+/+. Here EGFR−/− subclones represented subclones with no EGFR activating mutation and EGFR p.T790M mutation while EGFR+/+ represented subclones with EGFR activating mutation and EGFR p.T790M mutation. To calculate the contribution of the EGFR−/− subclones to the tumor volume, we first calculated the relationship between the VAF of EGFR-sensitive mutations and tumor volume in the progression of 12 patients and found

https://doi.org/10.1016/j.heliyon.2018.e01031

significant linearity between the tumor volume of these patients and the VAF of the EGFR-sensitive mutation. The linear relationship (y = 0.73103x - 0.55195) was then verified in 6 patients who later enrolled in this study, and the tumor volume at the time of drug resistance was simulated. Thus, the contribution of EGFR+/+ tumor subclones to the tumor volume was obtained. Finally, the true tumor volume minus the simulated tumor volume yields the contribution of EGFR−/− tumor subclones to the patient's tumor volume.

2.8.3. Other statistical analysis

Using the formula VAF/EGFR amplification*2 to adjust the VAFs of the EGFR point mutations, the adjusted VAF of EGFR mutation was then used for subsequent analysis. Pearson similarity was used to calculate the linear relationship between the VAF of the T790M mutant and VAF of the drug-sensitive mutation. In addition, Fisher's exact test and the Kolmogorov−Smirnov test were used to test the clinical distribution of baseline mutations between the EGFR p.T790M positive and negative groups, respectively, and the similarity of the resistance pattern between the two groups of EGFR-drug-sensitive mutations (EGFR p.19del vs. EGFR p.L858R).

All survival times and HRs in this study were calculated with their corresponding 95% CI values. All statistical tests were two-sided tests, and $P < 0.05$ indicates that the difference was statistically significant. All statistical analyses were performed using the R 3.3.0 toolkit.

3. Results

3.1. Baseline clinical and molecular characteristics of the patients

Fifty-three Chinese patients with advanced non-small cell lung cancer participated in our project. Their average age was 60 years. All patients had a clinical response to gefitinib (n = 28), erlotinib (n = 4), and icotinib (n = 21). We assessed tumor size changes in 46 patients with imaging data, 34 of who had measurable tumor foci after drug resistance. According to the drug response assessment (RECIST 1.1) manual standard [16], all 34 patients developed a strong drug resistance response (Fig. 1A). Among the 53 patients, 66.4% were treated with first-generation EGFR-TKIs as the first-line treatment. The median time to progression of 1st EGFR TKIs treatment was 7.4 months and ranged from 1.30 to 33.80 months. The baseline mutation profiles were detected in paraffin sections, tumor puncture samples, pleural effusions, and peripheral blood samples from all 53 patients (all samples were tested on the same platform and same gene target panel for mutation profile), among whom 8 also had cfDNA baseline mutation profiles measured using the NGS technique. During the entire course of treatment, the average number of cfDNA sampling was 1.86 in all patients, ranging from 1 to 6 times, and each patient

https://doi.org/10.1016/j.heliyon.2018.e01031

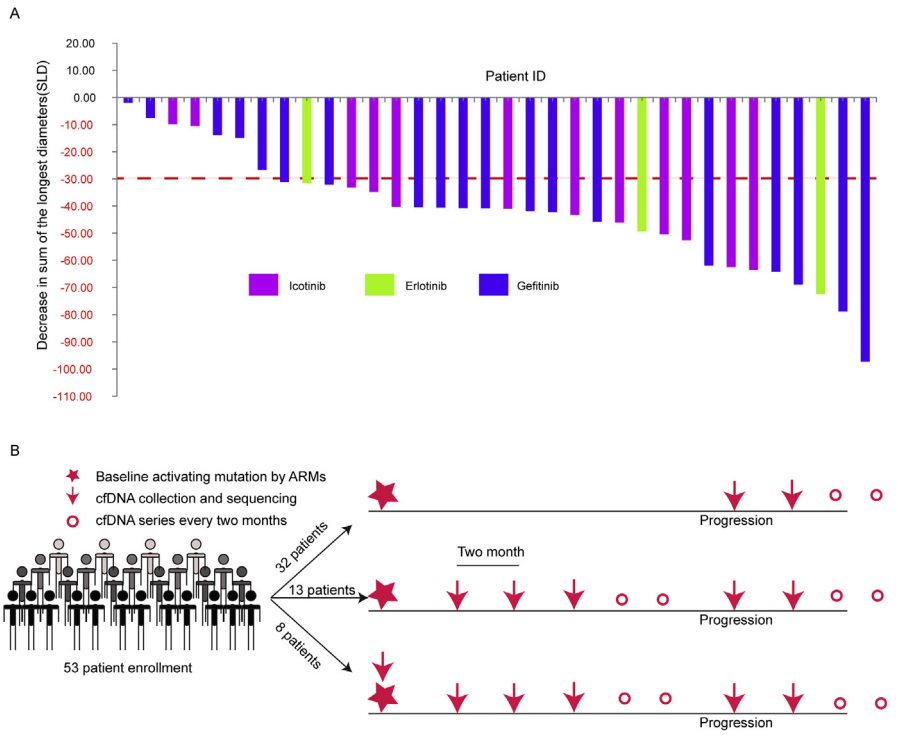

Fig. 1. Change of Sum of longest diameters (SLD) during from baseline to optimal response during 1st EGFR TKI treatment and summary of the temporal collection of liquid biopsies. (A) According to the standard of the Drug Reaction Assessment (RECIST 1.1) handbook, the red dotted line indicates that the tumor shrank by 30%, representing the drug clinical response of a PR. (B) 32 patients had first cfDNA liquid biopsies at progression. 13 patients started with ARMs method for baseline activating mutation detection and collection cfDNA samples at two-month interval until progression. 8 patients had baseline cfDNA samples and collected cfDNA samples at two month interval until progression. All patients kept collecting after progression at the same time interval if possible.

had at least one available mutation profile from ctDNA at the time of progression, which was summarized in Fig. 1B. The baseline drug-sensitive mutations detected in this study were EGFR p.19del and EGFR p.L858R, accounting for 67.92% and 32.08%, respectively. This baseline percentage was similar to that in previous studies [26, 27]. In addition, one patient was associated with EGFR L861Q and MET 14 skip mutations, one patient had both EGFR p.19del and EGFR p.L858R mutations, one patient had both EGFR p.19del and ALK fusion mutations, and one patient had both C-MET and EGFR p.L858R mutations. Other detailed clinical features are shown in Table 1.

3.2. CtDNA mutation profile and mutation load analysis

Among 53 pathologically confirmed NSCLC patients, the mean number of mutated genes was 3.79 in all cases and 7.13 for non-synonymous mutations. The number of mutations was significantly higher in 3 patients (P15, P16, P20) than in other patients (Fig. 2A). Of all the mutated genes, *EGFR* was the most commonly mutated gene,

https://doi.org/10.1016/j.heliyon.2018.e01031

Table 1. Clinical features of 53 NSCLC patients in China.

Clinical features	Clinical group	Number (percentage)
Age	Median	60 years
	Range	37−71 years
Age (%)	≤60	30 (56.6)
	>60	23 (43.4)
Sex (%)	Female	28 (52.83)
	Male	25 (47.17)
Stage	Stage IV	39 (73.5)
	Stage IIIb	2 (3.77)
	Recurrent	12 (22.64)
Histopathology (%)	Adenocarcinoma	47 (88.68)
	Squamous cell carcinoma	3 (5.66)
	Others	3 (5.66)
Smoking history (%)	Never smoker	41 (77.36)
	Ever smoker	12 (22.64)
EGFR mutation type (%)	19del	36 (67.92)
	21L858R	17 (32.08)
EGFR TKI line of treatment (%)	First line	35 (66.04)
	Second line	16 (30.19)
	Third line	2 (3.77)
EGFR TKI regimen	Erlotinib	4 (7.55)
	Gefitinib	28 (52.83)
	Icotinib	21 (39.62)

followed by *TP53*, *PDGFRA* and *BRCA2*. In addition, the frequency of other common drug resistance genes such as *KRAS, NRAS, PIK3CA, ERBB2, MET* was also higher in our patients (Fig. 2B), a finding that was consistent with previous study results in European and American patients [7]. Next, distribution of base substitution types of non-synonymous mutations was explored. Result showed that the dominant substitution types were C to T and G to A instead of substitution type: G to T caused by DNA damage [15] (Fig. 2C). This result was also consistent with previous study results and provided side-by-side support for the credibility of our acquired mutation data. After annotating the types of mutations, although *TP53, PDGFRA*, and *KIT* accounted for a high proportion of all mutations, no high-frequency repetitive mutations were found in these genes, suggesting that the somatic variation in these genes might not contribute much to drug resistance.

Most of the high-frequency repeated mutations were located in *EGFR, KRAS* and *NRAS* (Fig. 2D). In addition to the repeated EGFR p.T790M mutation and corresponding *EGFR* drug-sensitive mutation (EGFR p.19del, EGFR p.L858R) in *EGFR, KRAS* and *NRAS*, other high-frequency repetitive mutations were EGFR p.V769M, EGFR p.L747S, NRAS p.G60R and KRAS p.A11V (Fig. 2D). To our knowledge, KRAS p.A11V and EGFR p.V769M have not been previously reported. Among all patients, EGFR p.V769M was acquired in four patients at resistance (P5, P48, P61, P57), and only one patient had P57 with the EGFR p.T790M mutation,

https://doi.org/10.1016/j.heliyon.2018.e01031

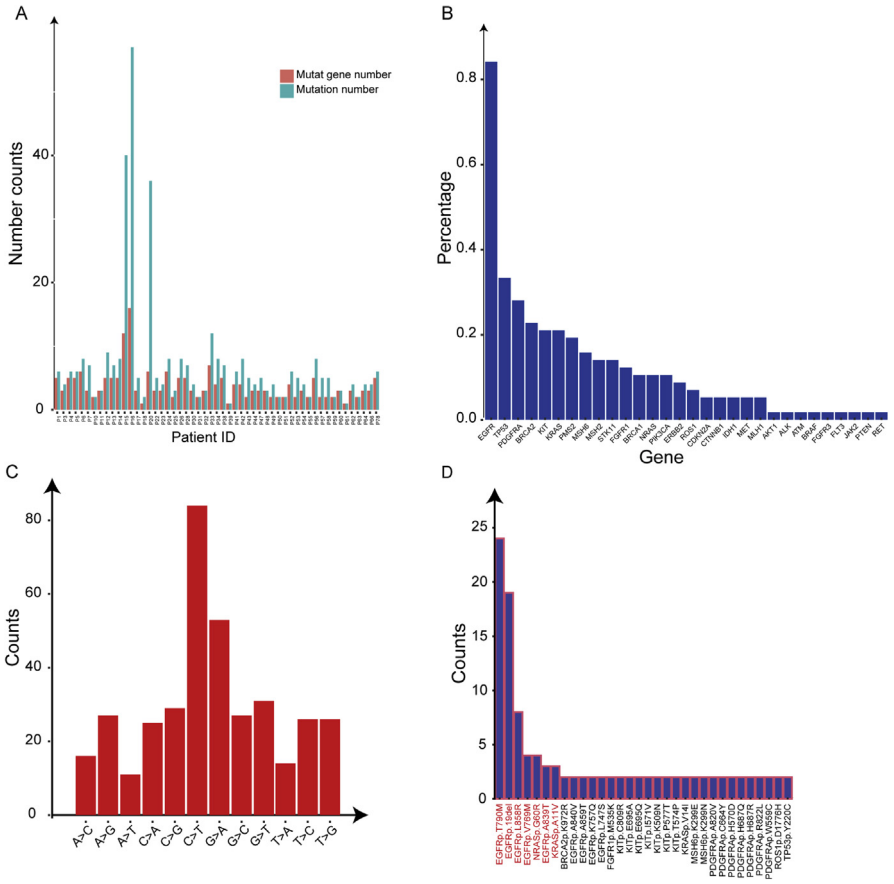

Fig. 2. Statistics of genes and mutations at drug resistance. (A) The number of mutant genes detected in all patients with resistance was marked in red, and the number of nonsynonymous mutations was marked in green. (B) Percentage distribution of mutant genes in all patients when resistant. (C) Distribution of base substitution types of non-synonymous mutations in all patients when resistant. (D) Recurrent non-synonymous mutation distribution in all patients.

indicating that there was no obvious correlation between the EGFR p.V769M mutation and drug-resistant mutation EGFR p.T790M, which belonged to two different tumor subclones. KRAS p.A11V mutations have been reported in gastric tissues and cancers and in hematopoietic and lymphoid tissues [28]. Three of the studied patients had this KRAS p.A11V mutation, but the mutation profiles were different; one had EGFR p.T790M (P57), one had a EGFR point mutation but no EGFR p.T790M (P48), and one had no *EGFR* mutation (P44), indicating no significant correlation between the KRAS p.A11V mutation and drug-resistant mutation EGFR p.T790M. Moreover, these mutations belonged to three different subclones. Furthermore, compared with the ctDNA mutation pattern before drug resistance (Fig. 3A for P5; Fig. 3B for P61; Fig. 3C for P48; Fig. 3D,E for P44), EGFR p.V769M and KRAS p.A11V were demonstrated to be acquired resistant mutations. Based on this observation, we suggested that these two new acquired mutations may be related to new drug resistance mechanisms and deserved further study.

https://doi.org/10.1016/j.heliyon.2018.e01031

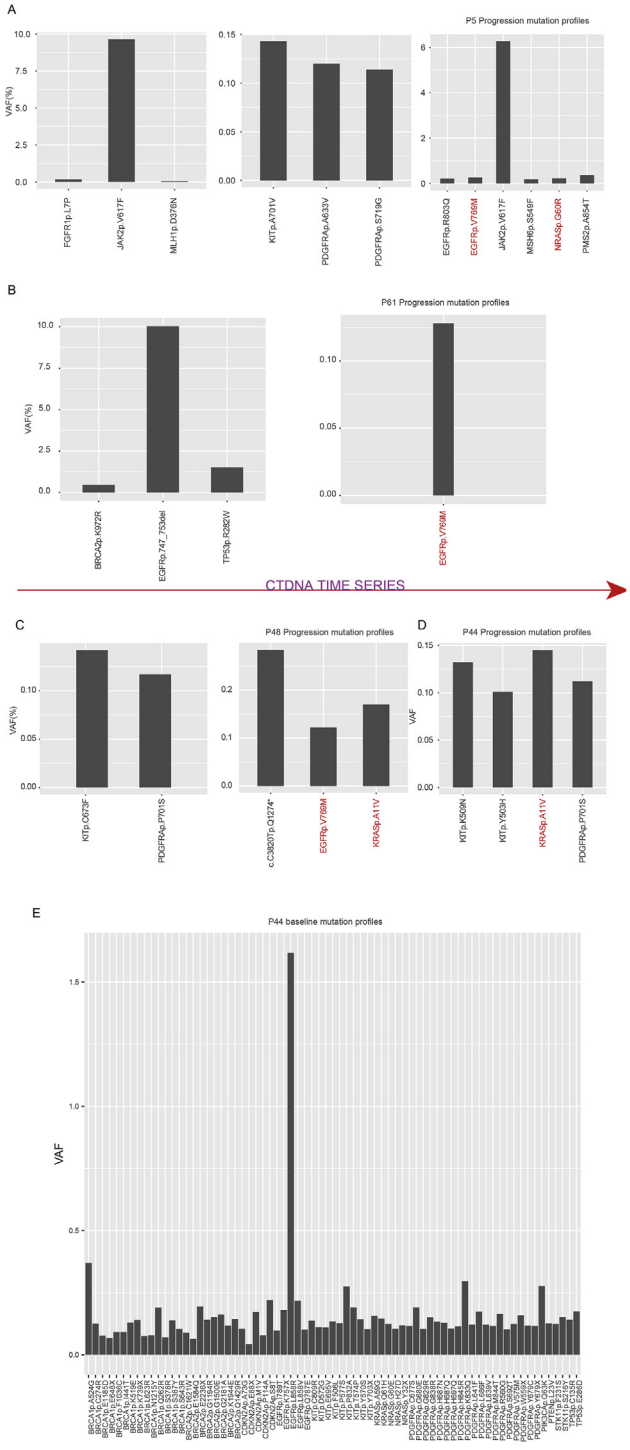

Fig. 3. Detailed mutation profiles of patients with EGFR p.V769M and KRAS p.A11V mutations. Recurrent and acquired mutations are marked in red during treatment. (A) The mutation profile of three ctDNA assays in P5. (B) Overview of two ctDNA series mutations in P61. (C) The mutation profile of two ctDNA assays in P48. (D) ctDNA mutation profile in progressive P44 with advanced disease. (E) Baseline ctDNA mutation profile in P44.

https://doi.org/10.1016/j.heliyon.2018.e01031

Based on tissue biopsy technology, the NSCLC acquired resistance mechanism study showed that the acquired EGFR p.T790M mutation is the most common mechanism of drug resistance, accounting for 40−50% of drug resistance cases [7]. We also obtained similar results from cfDNA samples from 53 NSCLC patients, with the EGFR p.T790M mutation accounting for 45.28% (Fig. 4A). In addition, our data showed two other high-frequency mutations that are significantly different from those in a previous study: *EGFR* point mutations (20.75%; Fig. 4A, pink wedges) and *KRAS/NRAS* point mutations (15.09%; Fig. 4A, dark red Wedge). In terms of amplification, 4 patients had *EGFR* amplification (P22: 3.06, P53: 3.8, P56: 10.6, P67: 3.59; 7.54%); one patient had *BRAF* amplification (P53: 4.25; 1.8%); and two patients had MET amplification (P53: 3.23, P67: 5.79; 3.7%), one of which was also associated with the EGFR p.T790M mutation. Previous studies based on Western populations have reported one patient with sensitive mutations of MET amplification with EGFR p.L858R after drug resistance [10]. A similar patient (P67) also appeared in our Chinese population. In addition, *ERBB2* amplification occurred only in one patient (P34: 4.23; 1.8%). In general, our *ERBB2* and *MET* amplification ratios were lower than those in previous studies [7].

The 1st TKI resistance studies showed that there are seven major drug resistance genes: E*GFR, KRAS, NRAS, MET, ERBB2, PIK3CA,* and *BRAF* [7]. Our study showed that in 53 patients, 49 acquired mutations occurred in at least one of the seven genes, with a proportion as high as 92.45%. According to the grouping of the 7 genes involved in the mutation, when resistant, 32.65% of 49 patients had acquired mutations in 2 or more genes, 24.49% had acquired a single mutation of a single gene, and 42.86% had acquired multiple mutations of a single gene (Fig. 4B). The proportion of drug-resistant mutations detected in this study was higher than those of previous tumor biopsy studies [8], indicating that liquid biopsy can obtain more comprehensive information than tissue biopsy when detecting resistance mutations. VAF values of all nonsynonymous mutations and the copy number change (CNA) of 49 patients in 7 resistant genes ranged between 0.045% and 91.64% (Fig. 4C). Among the 49 patients, we found that the mutation burden of these 7 drug resistance genes was significantly higher in 3 patients (P15, P16 and P20; Fig. 4C, marked red) than in the other patients. Compared with their own baseline mutation profiles (Supplementary Table 1), P15 and P20 acquired EGFR p.T790M mutations and other mutations in *KRAS* and *NRAS*, while P16 acquired mutations in *EGFR, KRAS, NRAS, PIK3CA, MET,* and *ERBB2*. The clinical response to 1st TKI treatment in these patients was poor, and pleural effusions recurred during treatment (PD and SD; Fig. 5). Clinically, their prognosis was significantly poor, and drug resistance developed rapidly. The above results indicated that the effect of treatment on NSCLC patients with 1st EGFR TKIs depended to some extent on the mutation number and the coverage and complexity of the mutation

https://doi.org/10.1016/j.heliyon.2018.e01031

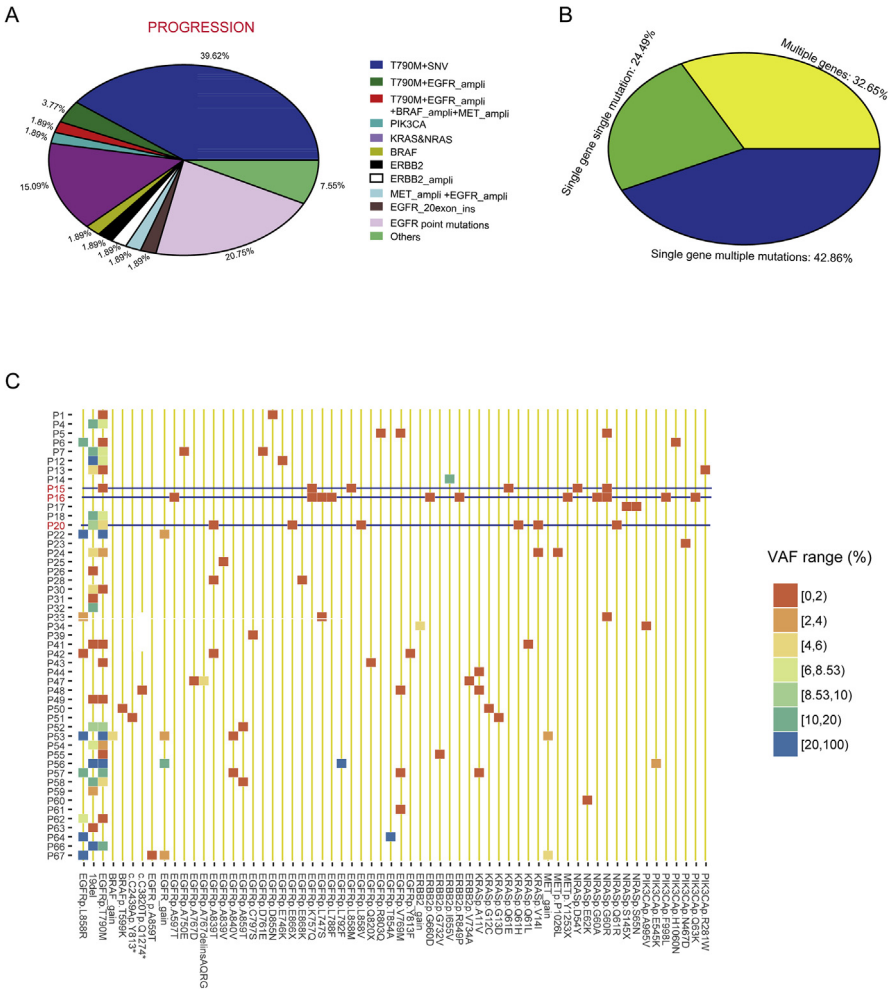

Fig. 4. Drug resistance mutation profile. (A) Acquired resistance mutant pie at the time of progression. Compared with the baseline mutation profile, the percentage of acquired resistance mutations was described. The blue wedge indicates the proportion of acquired EGFR p.T790M mutations accompanied with other point mutations. The dark blue wedge represents the EGFR p.T790M mutation with EGFR amplification. The red wedge represents the EGFR p.T790M mutation accompanied with EGFR and ERBB2 gene amplification. The bright green wedge represents the proportion of non-synonymous mutations in the *PIK3CA* gene. The dark red wedge represents the proportion of non-synonymous mutations in *KRAS* and *NRAS* genes. The yellow wedge indicates the proportion of non-synonymous mutations in *BRAF* gene. The black wedge represents the proportion of non-synonymous mutations in ERBB2 gene and the white wedge represents the mutation ratio of ERBB2 gene amplification. The pale green wedge represents the ratio of mutations in *MET* gene amplification and *EGFR* gene amplification. The gray wedge represents the insertion mutation ratio of the 20 exons of the *EGFR* gene. The pink wedge indicates the proportion of EGFR point mutations that do not contain EGFR p.T790M. (B) Statistical pie chart of multi-gene resistance mutation. The yellow wedge indicates the proportion of mutations that occur in multiple genes. The green wedge indicates that multiple mutation ratios occur in a single gene. The blue wedge indicates a single mutation in a single gene. (C) Heat maps of the VAF values for resistance mutations in 49 patients. The patient ID is the y-axis, and the corresponding amino acid change is the x-axis. Three patients with extremely high mutation counts are marked with the blue line.

https://doi.org/10.1016/j.heliyon.2018.e01031

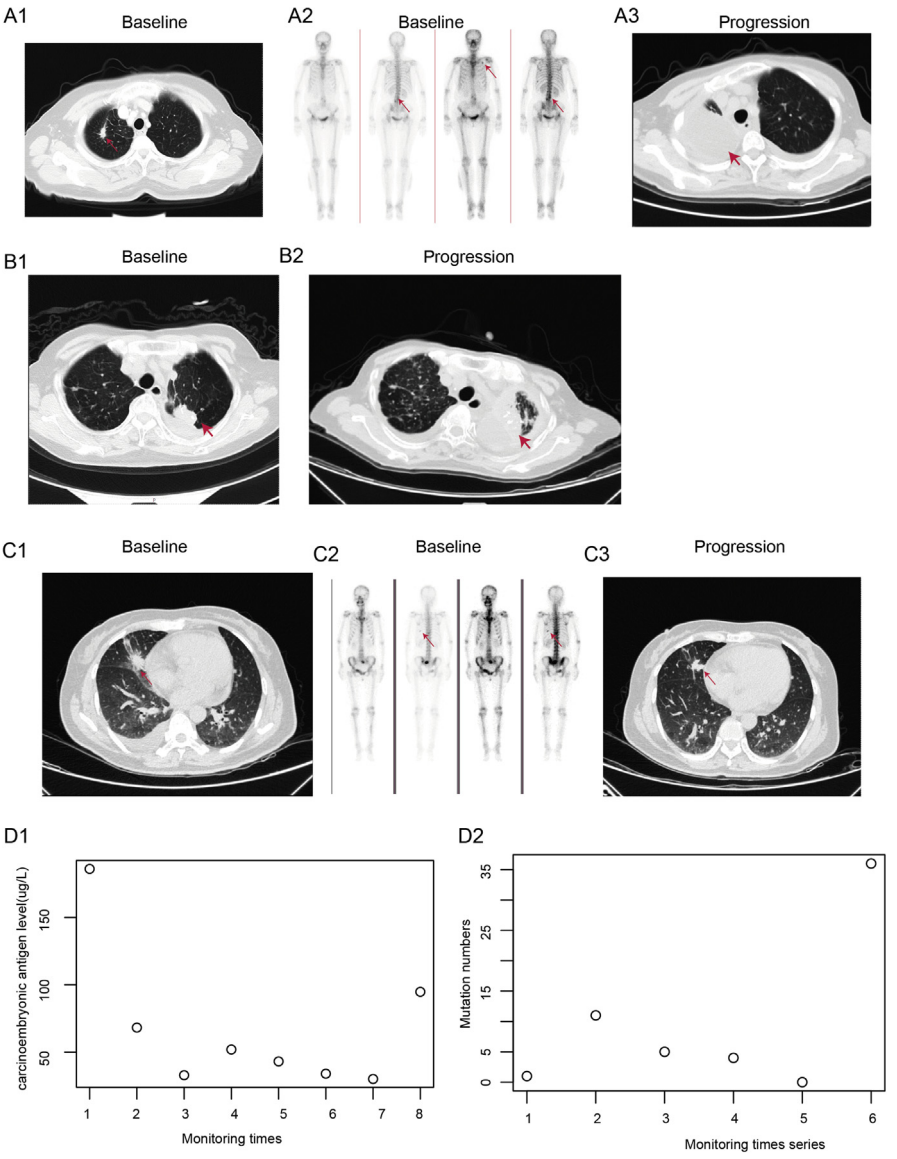

Fig. 5. Clinical data of 3 patients with an extremely high mutation burden. (A1, A2) Prior to 1st EGFR TKI treatment, P15 had small tumor foci with bone metastases. (A3) After progression, the ctDNA mutation profile showed an extremely high mutation burden and the corresponding tumor foci filled the entire right lung. (B1) Prior to 1st EGFR TKI treatment, P16 showed small tumor foci in the left lung with bone metastases. (B2) After progression, the ctDNA mutation profile showed an extremely high mutation burden, and the corresponding tumor foci filled the entire left lung. (C1, C2) P20 with bone metastases had a smaller initial lesion. (C3) Larger tumor lesions at progression. (D1) The number of different ctDNA mutations in P20 at 5 time points. (D2) Carcinoembryonic antigen (CEA) was significantly increased during 1st EGFR TKI treatment, and the change in CEA paralleled the number of point mutations.

load on the major drug resistance genes. In other words, this effect depended on the complexity and dynamic evolution of the subclone of tumors. The lower the mutation load was, the simpler the subclone composition and evolution pattern and the better the prognosis would be.

https://doi.org/10.1016/j.heliyon.2018.e01031

3.3. Two patient groups and mutation profiles of EGFR

Previous studies have shown that patients with EGFR p.L858R mutations detected in tumors and plasma have significantly shorter PFS [27, 29]. The same trend was also found in our clinical data (Fig. 6A, 4.1 months 95% CI: 3.1 to 13.4 and 10.7 months: 95% CI: 7.07 to 17.4; P = 0.004). In addition, we found that patients with the EGFR p.19del baseline mutation had a better 1st TKI clinical response than patients with the EGFR p.L858R baseline mutation (Fig. 6B, P = 0.034). This difference in PFS and 1st EGFR TKIs responses also affected the mutation profiles of the two baseline patient groups. By directly comparing the resistance mutation profiles of the two patient groups after drug resistance (Fig. 6C for EGFR p.19 del; Fig. 6D for EGFR p.L858R), although both groups had similar overall mutation profiles (P = 0.99), the highest-frequency mutations were located in the EGFR gene in both groups. However, the *EGFR* mutation load was significantly higher in the EGFR p.19del group than in the EGFR p.L858R group (23.9% vs. 14.9%). Specifically, the percentage of EGFR p.T790M mutations in patients with EGFR p.19del baseline mutations was significantly higher than that of EGFR p.L858R baseline mutations (62.1% vs. 19.3%, P = 0.007; Fig. 6E). Whether or not the *EGFR* baseline mutation spectrum determines the occurrence of EGFR p.T790M acquired

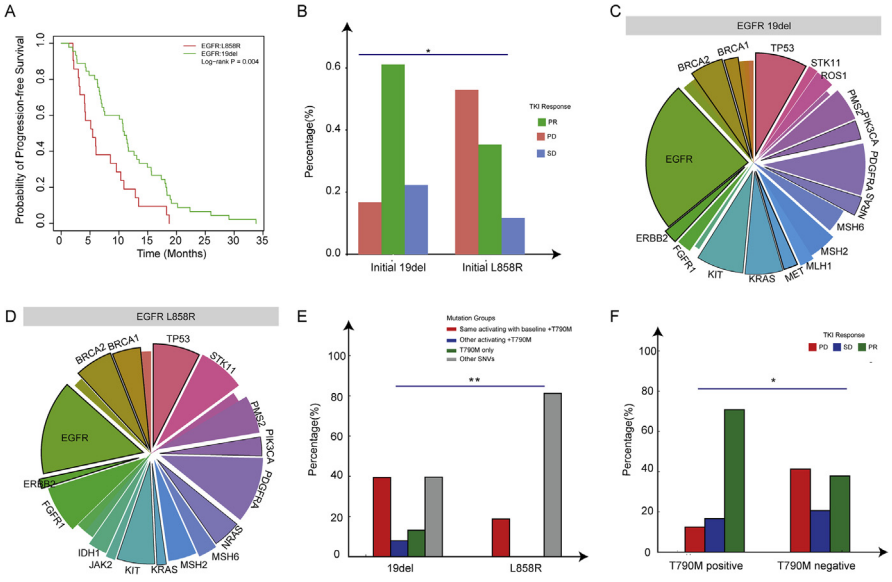

Fig. 6. Mutation profile and clinical features between two baseline mutation patient groups. (A) Kaplan-Meier plot without progression between baseline EGFR drug-sensitive mutation patient (19del vs. L858R) groups. (B) Distribution of 1st TKI clinical response between two baseline-mutated patient groups (* indicates P < 0.05 between the two groups). (C) Acquired resistant mutational pie chart for patient group with baseline EGFR p.19del mutation. (D) Acquired resistance mutation pie chart in the patient group with baseline EGFR p.L858R mutation. (E) Acquired EGFR p.T790M mutation ratio distribution between two patient groups with baseline EGFR drug-sensitive mutations (19del vs. L858R, ** indicates P < 0.01). (F) Distribution of 1st TKI clinical response between EGFR p.T790M positive and negative patient groups at progression (* indicates P < 0.05 between the two groups).

https://doi.org/10.1016/j.heliyon.2018.e01031

mutations has been controversial in previous studies [26, 30, 31], so we further calculated the clinical covariates of the EGFR p.T790M group and non-EGFR p.T790M group and found that the type of baseline mutation in the patient did indeed determine the occurrence of the EGFR p.T790M mutation to a large extent. Our clinical data showed that in patients with a better prognosis, the incidence of acquired mutations of EGFR p.T790M was higher (the proportions in the EGFR p.19del and EGFR p.L858R groups were 62.1% and 19.3%, respectively; P = 0.007). From the above perspective, by analyzing the baseline mutation profiles of NSCLC patients, we could know the dynamic evolution of tumor subclones during 1st EGFR TKIs treatment, and then it could be possible to predict the therapeutic effect of 1st EGFR TKIs. In addition, we found a significant difference in the baseline mutations in other genes between the two groups (Fig. 6C and D). For example, the frequency of KRAS and NRAS mutations was significantly higher in the 19del patient group than in the L858R patient group (8.8% vs. 5.8%).

Our data showed that the patients had the highest frequency of *EGFR* mutations. Forty-two patients had *EGFR* mutations (Fig. 7A). Some of the mutation patterns have previously been reported: EGFR p.T790M (24 patients), EGFR p.L747S (2 patients) [32], EGFR p.T854A (1 Patient) [33], and one EGFR exon insertions (1 patient) [33]. In addition, 3 of 4 *EGFR* CNA-amplified patients (P22, P53, P56 and P67) were simultaneously associated with acquired EGFR p.T790M mutations (P22, P53 and P56) (3.77%; Fig. 4A: dark blue wedges). Most of the baseline drug-sensitive mutations persisted after drug resistance. Compared with the group without the EGFR p.T790M mutation, sensitive mutations appeared at high frequencies in the EGFR p.T790M-containing group (Fig. 7A is separated by a dash-dark purple line; 52.6% vs. 87.5%, P = 0.0032; Baseline drug sensitive mutations were marked in red). This phenomenon has also been reported in previous studies [10]. In addition, based on the feature of the quantification of mutated profiles by NGS-based ctDNA detection, we found for the first time that there was a significant linear relationship between the VAFs of the EGFR p.T790M and drug-sensitive mutations observed during the stage of drug resistance ($y = 1.0709x + 5.8622$; $r = 0.68$, $p = 0.00025$, Fig. 7B).

The reasons were as follows: 1) patients with the EGFR p.19del baseline mutation had a better clinical response than those with the EGFR p.L858R baseline mutation to 1st EGFR TKIs, 2) after drug resistance, drug-sensitive mutations occurred at a high frequency in patients with EGFR p.T790M mutations, and 3) the clinical data showed that in patients with a better prognosis, the incidence of acquired EGFR p.T790M mutations was significantly higher (Fig. 6F). Combined with the observed significant linear relationship between the VAFs of the EGFR p.T790M and drug-sensitive mutations, we concluded that the existence and evolution of EGFR p.19del/p.L858R + EGFR p.T790M subclones suggested not only that 3rd EGFR TKIs therapeutic agents could be used for the subsequent treatment of

https://doi.org/10.1016/j.heliyon.2018.e01031

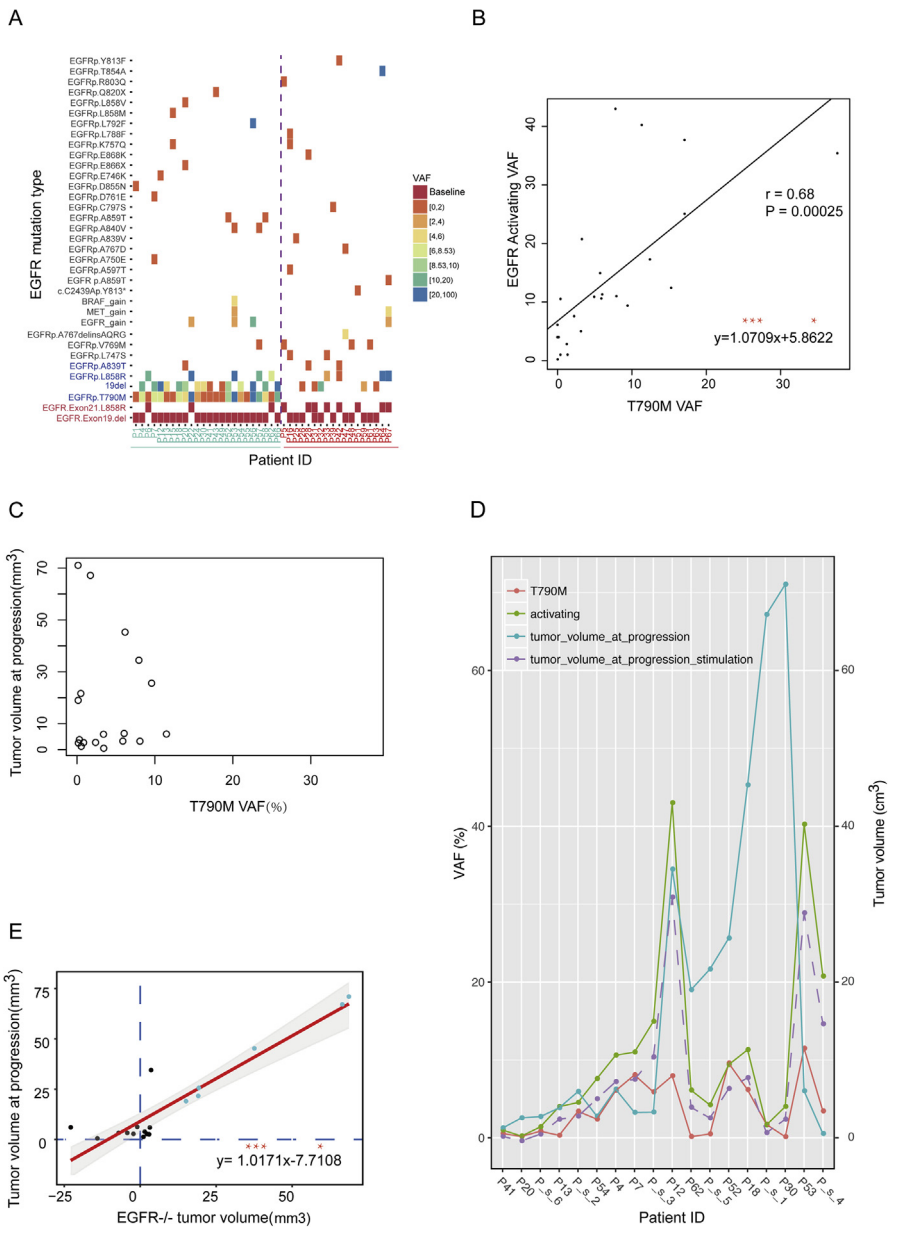

Fig. 7. Analysis of the EGFR mutation profile between the EGFR p.T790M positive and negative patient groups and analysis of the relationship between the VAF of the EGFR mutations and tumor size. (A) A heat map of the VAF of the EGFR gene mutation in the 42 patients after drug resistance. (B) Linear relationship between the VAF of EGFR drug-sensitive mutations and VAF of EGFR p.T790M after resistance in 21 patients ($r = 0.68$, $p = 0.00025$). (C) The VAF of EGFR p.T790M versus tumor size in 18 patients after drug resistance ($r = 0.22$, $P = 0.48$). (D) The VAF of EGFR drug-sensitive mutations and VAF of EGFR p.T790M in 18 patients and tumor volume maps in resistance. The red line represents the VAF value of EGFR p.T790M in 18 patients. Dark green indicates the VAF of EGFR drug-sensitive mutations. Light green represents the tumor volume at drug resistance. The purple dotted line represents the estimated tumor volume. (E) Estimated linear relationship between the ratio of EGFR −/− tumor subclones and tumor size in 18 EGFR p.T790M-positive patients ($y = 0.956x + 5.9465$; $r = 0.93$, $P = 2.2 * 10^{-8}$; The green dots represent the contributions from the tumor subclone EGFR −/−, and the black dots represent the contributions from the tumor subclone EGFR +/+).

https://doi.org/10.1016/j.heliyon.2018.e01031

patients who develop resistance but also that 3rd EGFR TKIs could be used as biomarkers to evaluate the efficacy of 1st EGFR TKIs therapy. Fortunately, our data showed that after 1st EGFR TKIs treatment, T790M-resistant mutations occurred in more than 50% of patients, and most of them also had EGFR p.19del/p.L858R mutations (71.42%, Fig. 7A). These patients not only had a good prognosis after 1st TKI treatment but also received follow-up treatment with 3rd TKI.

Finally, we investigated the correlation between disease phenotypes and mutation profiles during cancer treatment and found that the VAF of EGFR p.T790M was not associated with the tumor volume when resistant ($r = 0.22$, $P = 0.48$; Fig. 7C). The clinical data also showed that during treatment, tumor progression seems unlikely to be associated with the drug resistance caused by the T790M mutation. However, due to the significant linear relationship between activating mutation and acquired T790M and validation of same allele harboring T790M and activating mutation by previous research [34], we discovered two major tumor clones, namely, clone EGFR +/+ (activating mutation and EGFR p.T790M; Fig. 7D, 10 patients) and clone EGFR −/− (no activating mutation and no EGFR p.T790M mutation; Fig. 7D, 6 patients), which played different roles in tumor progression and prognosis. In patients with a high proportion of EGFR +/+ clones, the tumor volume did not correlate with changes in the VAF of the EGFR p.T790M mutant. Patients with a high proportion of the EGFR −/− clone showed a relatively large tumor volume that was proportional to the ratio of the EGFR −/− clone (Fig. 7E, points marked green, $y = 1.0171x - 7.7108$; $r = 0.93$, $P = 2.2 * 10\text{-}8$). The results showed that the EGFR −/− tumor clone appeared to play a more important role in tumor resistance than the EGFR +/+ clone and that the EGFR−/− tumor clone has a greater impact on prognosis. Follow-up treatment data also support our conclusions (Supplementary Table 3, 87.5% PR response in EGFR +/+). In advanced patients, we found that patients with a predominant EGFR−/− clone had a worse prognosis than those with EGFR +/+ clones (Supplementary Table 3, 0.0% PR response in EGFR −/−).

3.4. Multitime ctDNA dynamic analysis shows spatial and temporal diversity of the EGFR p.T790M mutation

Because cfDNA sampling had a minimally invasive advantage, the cfDNA liquid biopsy technique can play an important role in dynamically monitoring the tumor state and has significant clinical value [18]. Here, through dynamic tracking and multi-time cfDNA analysis, we obtained interesting cases that showed the temporal and spatial diversity of multiclonal evolution in tumor tissues throughout 1st EGFR-TKIs treatment and could help us make appropriate treatment decisions.

In these cases, P50 did not acquire EGFR drug-sensitive mutations prior to enrollment. Chemotherapy was her first-line treatment option. After resistance to

https://doi.org/10.1016/j.heliyon.2018.e01031

chemotherapy developed, the resulting ctDNA mutation profile showed that the patient developed EGFR p.19del (Fig. 8A green line) drug-sensitive mutations. When the tumor was resistant to 1st EGFR-TKI treatment (black dashed line in Fig. 8A), P50 acquired the KRAS p.G12C mutation [35] (VAF = 0.0023, Fig. 8A blue line), while the EGFR p.19del mutation disappeared. At this stage, although there was no major change in the tumor volume (1.7 cm−1.71 cm), bone metastases occurred in P50. Chemotherapy was then used again as a third-line treatment, and the ctDNA mutation profile was captured again after the third-line chemotherapy.

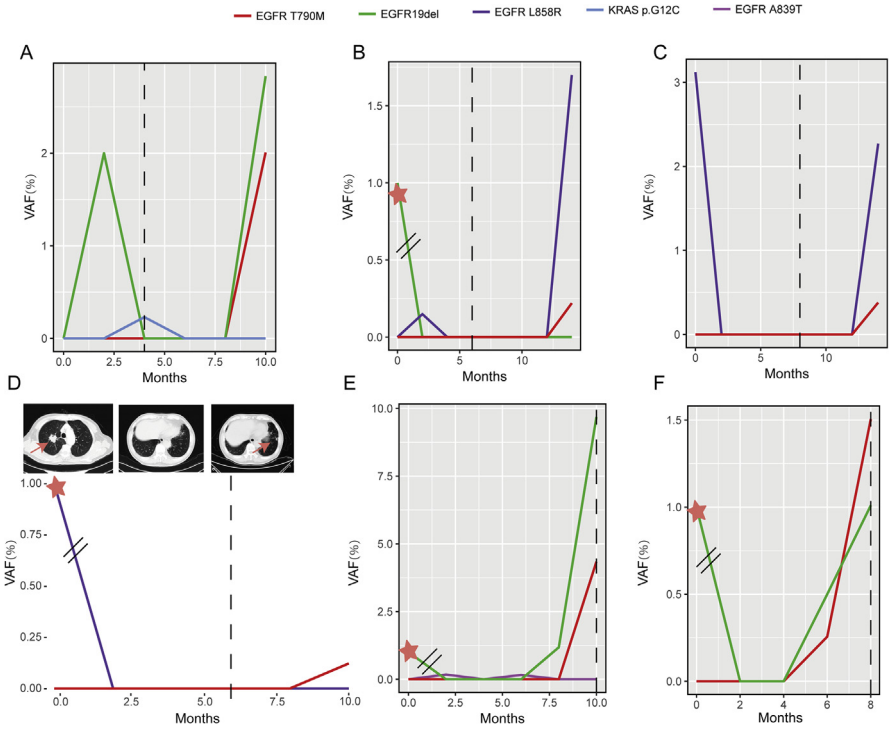

Fig. 8. Dynamic analysis of ctDNA revealed spatial and temporal diversity of EGFR p.T790M mutations. Throughout the monitoring process, the red line represents the mutation trend of EGFR p.T790M, the green line represents the mutation trend of EGFR p.19del, the blue line represents the mutation trend of EGFR p.L858R, the light blue line represents the mutation trend of KRAS p.G12C, and the dark red line represents the mutation trend of EGFR p.A839T. The black dashed lines indicate the time points of drug resistance, the red stars indicate baseline drug-sensitive mutations as detected by the ARMs method. (A) The EGFR p.T790M mutation occurred in the sixth month after pathologically confirmed resistance in P50. (B) The EGFR p.T790M mutation occurred in the eighth month after pathologically confirmed resistance in P39. (C) The EGFR p.T790M mutation occurred in the sixth month after pathologically confirmed resistance in P60. (D) P5 received 1st EGFR TKI treatment as an adjunctive treatment after surgery, and new metastatic lesions appeared in the left lung during drug resistance. Four months later, an EGFR p.T790M mutation was observed. (E) P20 showed that the EGFR p.T790M mutation occurred in the early treatment phase and was then inhibited and eventually disappeared in drug resistance. At the same time, P20 also demonstrated three mutation trends of the EGFR gene and the corresponding competitive evolution of tumor subclones. (F) P49 showed that EGFR p.T790M appeared 2 months prior to pathologically confirmed drug resistance, and the VAF value rose further when resistant.

https://doi.org/10.1016/j.heliyon.2018.e01031

Finally, we captured EGFR p.T790M (Fig. 8A red line) and EGFR p.19del (VAF 0.0208 and 0.0283, respectively) mutations in EGFR, according to which the patient was treated with 3rd EGFR-TKIs, and the prognosis was good.

The baseline sensitive mutation in P39 was EGFR p.19del. After two months of 1st EGFR TKIs treatment, the ctDNA mutation profile showed the appearance of EGFR p.L858R, while the VAF of EGFR p.19del dropped to zero (Fig. 8B green and blue lines), indicating that the polyclonal components of the original tumor tissue underwent competitive evolution. At the time of progression, no drug-related mutations were detected, and the EGFR p.L858R mutation disappeared. Subsequent monitoring of the EGFR p.T790M mutation was observed, and the EGFR p.L858R mutation also reappeared (VAF values of 0.22 and 1.7, respectively), again suggesting that the 3rd EGFR-TKI targeted therapy timing was ideal for this patient. The phenomenon that EGFR p.T790M did not appear immediately after drug resistance also occured in P60. At the advanced stage, no known drug resistance-related mutations were detected in the ctDNA mutation profile of P60. After 4 consecutive follow-up detections, the EGFR p.T790M mutation was finally detected (Fig. 8C, red line). The condition of P5 was different, showing spatial and temporal complexity of the EGFR p.T790M mutation. EGFR-TKI was used as adjuvant treatment for surgical removal of the right lung mass. After 2 months of treatment, the ctDNA mutation profile showed that the VAF of EGFR p.L858R was reduced to zero. At the advanced stage, no EGFR p.T790M and drug sensitivity mutations were found. However, when a new metastatic lesion appeared in the left lung, the EGFR p.T790M mutation appeared, with a VAF of 0.00122 (Fig. 8D, red line) and prompted the intervention of the 3rd EGFR TKIs targeted therapy. In these four cases, ctDNA mutation monitoring provided a basis for subsequent accurate treatment of NSCLC patients.

The other two patients (P20, P49) showed that the appearance of the EGFR p.T790M mutation was earlier than that of clinical drug resistance, and the EGFR drug-sensitive mutations in P20 occurred alternately, indicating the time complexity of tumor polyclonal evolution during 1st EGFR-TKIs treatment. P20 developed an EGFR p.T790M mutation early in treatment with a VAF of 0.0017. Multiple subsequent EGFR drug-sensitive mutations occurred successively during treatment. The tumor subclone containing the EGFR p.19del mutation first disappeared, the VAF decreased to 0, another tumor subclone carrying the EGFR p.A839T mutation began to appear, and the VAF of the EGFR p.A839T mutation decreased from 0.00174 to 0.0016 and then decreased to zero (Fig. 8E, dark red line). Immediately following the reappearance of tumor subclones containing the EGFR p.19del mutation, the VAF increased from 0 to 0.0118 and then increased to 0.0968 (Fig. 8E, green line). At the same time, subclones of the tumor containing the EGFR p.T790M mutation appeared, and the VAF increased to 0.0434 (Fig. 8E red line).

https://doi.org/10.1016/j.heliyon.2018.e01031

For P49, we analyzed ctDNA data from four monitoring sites before drug resistance. The EGFR p.T790M mutation occurred at the third and fourth detection time points with VAF values of 0.0025 and 0.0015, respectively, and the time at which the clinical drug resistance occurred coincided with the time of the fourth test (Fig. 8F), indicating that the time of appearance of the clinical resistance phenotype after 1st TKI treatment was not completely consistent with the time of appearance of the EGFR p.T790M mutation.

These examples showed that ctDNA technology could clearly reveal the complex dynamic spatiotemporal diversity of tumor clones and that the dynamic information obtained was of great significance to enable correct treatment decisions after EGFR-TKI resistance.

4. Discussion

In this work, we used a NGS technology based cfDNA liquid biopsy technique for 53 Chinese patients with NSCLC to study their resistance mechanism after treatment with 1st EGFR TKIs. This is a liquid biopsy study of the drug resistance mechanism of NSCLC with the largest sample size in China so far. Our research shows that the mutation spectrum presented by Chinese NSCLC patients in drug resistance covers almost all reported resistance mutations based on tissue samples and has similar frequency of mutations. It shows that the liquid biopsy technique is feasible and reliable in obtaining effective tumor mutation data. In addition, our study shows that liquid biopsy can better overcome the incompleteness of the data obtained due to tumor heterogeneity. Further, due to the non-invasive advantages, we can see from this study that liquid biopsy technology can conveniently and long-termly obtain the prognosis-associated mutation spectrum of patients, thus giving detailed information on the composition and evolution of tumor clones.

Not surprisingly, our data show that the greatest contribution to drug resistance still comes from secondary EGFR p.T790M point mutations, consistent with previous studies, ranging from 40% to 63% [7, 8, 10]. What is worth proposing is some newly discovered inconsistencies. Compared with previous work, in addition to the common resistance mechanisms, our data also showed some inconsistent results. Sequist, L.V proposed *PIK3CA* (5%) as a drug resistance gene, accompanied by T790M point mutation, EGFR amplification and small cell lung cancer (SCLC) transformation [10], Yu, H.A observed in his work a higher frequency of MET amplification and SCLC transformation accompanied by a T790M point mutation. None of them detected *PIK3CA, KRAS, NRAS, ERBB2* and infrequent *EGFR* point mutations [8]. In our patients, we detected high-frequency point mutations in *KRAS* and *NRAS* and *EGFR*. The MET amplification in our cohort was found only in two patients (3.77%), one of who was accompanied by a T790M point mutation.

https://doi.org/10.1016/j.heliyon.2018.e01031

In other studies, the frequency of MET amplification was generally less than 15−20% [36, 37]. A few studies support this result. Previous two prospective studies get the similar results (2 of 37; 4 of 75 [8, 10]). We cannot easily explain this lower than expected mutation frequency, and an accurate percentage of MET amplification require further larger patient cohort assessments. EGFR p.T790M point mutation was the second large resistance mutation (33.9%). A review showed that 1%−2% other point mutation in EGFR were emergent in the process of drug resistant to 1st EGFR TKI treatment in some cases of cohort study [7]. Previous Taiwan cohort study also shows a high frequency of other point mutations in EGFR [38].

Another important feature of this study is the deep integration of disease phenotype information and liquid biopsy data. The integration of patient clinical information and genomics data enables us to conduct supervised data analysis and clearly describe the evolutionary process of different tumor clones and their relevance to drug resistance. We have found that in the course of drug resistance, the complexity and spatiotemporal diversity of tumor clones determine the efficacy and prognosis of treatment, the composition and competitive evolution of tumor clones have a decisive influence on treatment, and the competitive evolution of tumor clones can be adjusted by targeted drugs and chemotherapy. These findings may have new implications for the clinical treatment of patients with NSCLC.

In the drug resistance process, for most Chinese patients, there exist two major tumor clones, EGFR−/− (activating- and T790M-) and EGFR+/+ (activating+ and T790M+). The competitive evolution of these two tumor clones, which cause complexity of the resistance mechanism and the uncertainty of the prognosis. Our experiment data and calculations show that the contribution of tumor clone anchored with EGFR−/− to drug resistance and prognosis is significantly worse than that of tumor clone with EGFR+/+ for third generation TKI therapy.

It shows that it is important to adjust the treatment according to tumor clone constitution [10]. If we further subdivide, some of the tumor sub-clones can be found in the stage of drug resistance. Of them three important sub-clones were found, these sub-clones are in addition to be anchored with an common novo mutation KRAS A11V, one with EGFR p.T790M point mutation, one with EGFR point mutation without T790M, one without any EGFR mutation. Based on this observation it looks like a new tumor clone anchored with KRAS p.A11V point mutant appear significantly. Another sub-clone anchored with a new EGFR p.V769M point mutation has been also found in the process of drug resistance. Previous research showed EGFR p.V769M was acquired in only one Chinese patient [38]. In our study EGFR p.V769M was appeared in four patients and only one with T790M mutations (P57). In our view, these two novo mutations are likely to be associated with a new drug resistance mechanism and are worth further study.

https://doi.org/10.1016/j.heliyon.2018.e01031

The evolution process of tumor clones is always a question worth studying and fascinating [39]. For a number of patients, through the dynamic tracking and dynamical cfDNA analyzing, we have got some interesting cases, which show the spatiotemporal diversity of the clinically meaningful cancer treatment. In these cases, the major drug resistance mutation EGFR p.T790M and the drug sensitive mutation EGFR p.19del repeatedly and alternately appeared in the course of drug resistance, it is either bound or not bound to other resistance mutations during the process of drug resistance. The temporal and spatial dynamic complexity of this clonal evolution continues to provide new opportunities for NSCLC targeted therapy, which can really help us make appropriate treatment decisions.

Despite some limitations, the multiple resistance mechanism of 1st EGFR TKI in Chinese population was studied; our findings are useful for the discovery of new drug resistance mechanisms, as well as understanding the clinical implications of the composition and evolution of tumor clones.

Declarations

Author contribution statement

Qinfang Deng, Boxiong Xie, Xianxiu Ji, Qiyu Fang, Yuchen Bao, Jialu Li, Shengnan Jin, Chunming Ding: Performed the experiments; Contributed reagents, materials, analysis tools or data.

Leilei Wu: Analyzed and interpreted the data; Wrote the paper.

Chao Li, Li Feng: Analyzed and interpreted the data.

Yixue Li, Songwen Zhou: Conceived and designed the experiments.

Funding statement

This work was supported by National Key R&D Program of China (2017YFA0505500, 2016YFC0901704, 2017YFC0907505 and 2017YFC0908405), National Natural Science Foundation of China (81301994) and National High-Tech R&D Program (863) (2015AA020105).

Competing interest statement

The authors declare no conflict of interest.

Additional information

Supplementary content related to this article has been published online at https://doi.org/10.1016/j.heliyon.2018.e01031.

Acknowledgements

We appreciate Smartquerier Co., Ltd for provided designed panel and analyses.

References

[1] A. Inoue, T. Suzuki, T. Fukuhara, M. Maemondo, Y. Kimura, N. Morikawa, H. Watanabe, Y. Saijo, T. Nukiwa, Prospective Phase II study of gefitinib for chemotherapy-naïve patients with advanced non−small-cell lung cancer with epidermal growth factor receptor gene mutations, J. Clin. Oncol. 24 (2006) 3340−3346.

[2] L.V. Sequist, R.G. Martins, D. Spigel, S.M. Grunberg, A. Spira, P.A. Jänne, V.A. Joshi, D. McCollum, T.L. Evans, A. Muzikansky, G.L. Kuhlmann, M. Han, J.S. Goldberg, et al., First-line gefitinib in patients with advanced non−small-cell lung cancer harboring somatic EGFR mutations, J. Clin. Oncol. 26 (2008) 2442−2449.

[3] R. Rosell, E. Carcereny, R. Gervais, A. Vergnenegre, B. Massuti, E. Felip, R. Palmero, R. Garcia-Gomez, C. Pallares, J.M. Sanchez, Erlotinib versus standard chemotherapy as first-line treatment for European patients with advanced EGFR mutation-positive non-small-cell lung cancer (EURTAC): a multicentre, open-label, randomised phase 3 trial, Lancet Oncol. 13 (2012) 239−246.

[4] T. Mitsudomi, S. Morita, Y. Yatabe, S. Negoro, I. Okamoto, J. Tsurutani, T. Seto, M. Satouchi, H. Tada, T. Hirashima, Gefitinib versus cisplatin plus docetaxel in patients with non-small-cell lung cancer harbouring mutations of the epidermal growth factor receptor (WJTOG3405): an open label, randomised phase 3 trial, Lancet Oncol. 11 (2010) 121−128.

[5] D.H. Lee, Treatments for EGFR-mutant non-small cell lung cancer (NSCLC): the road to a success, paved with failures, Pharmacol. Ther. (2017).

[6] M.J. Niederst, L.V. Sequist, J.T. Poirier, C.H. Mermel, E.L. Lockerman, A.R. Garcia, R. Katayama, C. Costa, K.N. Ross, T. Moran, RB loss in resistant EGFR mutant lung adenocarcinomas that transform to small-cell lung cancer, Nat. Commun. 6 (2015).

[7] D.R. Camidge, W. Pao, L.V. Sequist, Acquired resistance to TKIs in solid tumours: learning from lung cancer, Nat. Rev. Clin. Oncol. 11 (2014) 473−481.

[8] H.A. Yu, M.E. Arcila, N. Rekhtman, C.S. Sima, M.F. Zakowski, W. Pao, M.G. Kris, V.A. Miller, M. Ladanyi, G.J. Riely, Analysis of tumor specimens at the time of acquired resistance to EGFR-TKI therapy in 155 patients with EGFR-mutant lung cancers, Clin. Canc. Res. 19 (2013) 2240−2247.

https://doi.org/10.1016/j.heliyon.2018.e01031

[9] K. Suda, K. Tomizawa, M. Fujii, H. Murakami, H. Osada, Y. Maehara, Y. Yatabe, Y. Sekido, T. Mitsudomi, Epithelial to mesenchymal transition in an epidermal growth factor receptor-mutant lung cancer cell line with acquired resistance to erlotinib, J. Thorac. Oncol. 6 (2011) 1152−1161.

[10] L.V. Sequist, B.A. Waltman, D. Dias-Santagata, S. Digumarthy, A.B. Turke, P. Fidias, K. Bergethon, A.T. Shaw, S. Gettinger, A.K. Cosper, Genotypic and histological evolution of lung cancers acquiring resistance to EGFR inhibitors, Sci. Transl. Med. 3 (2011), 75ra26-75ra26.

[11] C. Yamamoto, Y. Basaki, A. Kawahara, K. Nakashima, M. Kage, H. Izumi, K. Kohno, H. Uramoto, K. Yasumoto, M. Kuwano, Loss of PTEN expression by blocking nuclear translocation of EGR1 in gefitinib-resistant lung cancer cells harboring epidermal growth factor receptor−activating mutations, Cancer Res. 70 (2010) 8715−8725.

[12] J. Zhang, J. Fujimoto, J. Zhang, D.C. Wedge, X. Song, J. Zhang, S. Seth, C.-W. Chow, Y. Cao, C. Gumbs, Intratumor heterogeneity in localized lung adenocarcinomas delineated by multiregion sequencing, Science 346 (2014) 256−259.

[13] E.C. de Bruin, N. McGranahan, R. Mitter, M. Salm, D.C. Wedge, L. Yates, M. Jamal-Hanjani, S. Shafi, N. Murugaesu, A.J. Rowan, Spatial and temporal diversity in genomic instability processes defines lung cancer evolution, Science 346 (2014) 251−256.

[14] J.J. Chabon, A.D. Simmons, A.F. Lovejoy, M.S. Esfahani, A.M. Newman, H.J. Haringsma, D.M. Kurtz, H. Stehr, F. Scherer, C.A. Karlovich, Circulating tumour DNA profiling reveals heterogeneity of EGFR inhibitor resistance mechanisms in lung cancer patients, Nat. Commun. 7 (2016).

[15] A.M. Newman, A.F. Lovejoy, D.M. Klass, D.M. Kurtz, J.J. Chabon, F. Scherer, H. Stehr, C.L. Liu, S.V. Bratman, C. Say, Integrated digital error suppression for improved detection of circulating tumor DNA, Nat. Biotechnol. 34 (2016) 547.

[16] E.A. Eisenhauer, P. Therasse, J. Bogaerts, L.H. Schwartz, D. Sargent, R. Ford, J. Dancey, S. Arbuck, S. Gwyther, M. Mooney, L. Rubinstein, L. Shankar, L. Dodd, et al., New response evaluation criteria in solid tumours: revised RECIST guideline (version 1.1), Eur. J. Cancer 45 (2009) 228−247.

[17] D.M. Euhus, C. Hudd, M.C. Laregina, F.E. Johnson, Tumor measurement in the nude mouse, J. Surg. Oncol. 31 (1986) 229−234.

[18] A.M. Newman, S.V. Bratman, J. To, J.F. Wynne, N.C. Eclov, L.A. Modlin, C.L. Liu, J.W. Neal, H.A. Wakelee, R.E. Merritt, J.B. Shrager,

https://doi.org/10.1016/j.heliyon.2018.e01031

B.W. Loo Jr., A.A. Alizadeh, et al., An ultrasensitive method for quantitating circulating tumor DNA with broad patient coverage, Nat. Med. 20 (2014) 548−554.

[19] H. Li, R. Durbin, Fast and accurate long-read alignment with Burrows−Wheeler transform, Bioinformatics 26 (2010) 589−595.

[20] H. Li, B. Handsaker, A. Wysoker, T. Fennell, J. Ruan, N. Homer, G. Marth, G. Abecasis, R. Durbin, The sequence alignment/map format and SAM tools, Bioinformatics 25 (2009) 2078−2079.

[21] Z. Lai, A. Markovets, M. Ahdesmaki, B. Chapman, O. Hofmann, R. McEwen, J. Johnson, B. Dougherty, J.C. Barrett, J.R. Dry, VarDict: a novel and versatile variant caller for next-generation sequencing in cancer research, Nucleic Acids Res. 44 (2016) e108.

[22] K. Cibulskis, M.S. Lawrence, S.L. Carter, A. Sivachenko, D. Jaffe, C. Sougnez, S. Gabriel, M. Meyerson, E.S. Lander, G. Getz, Sensitive detection of somatic point mutations in impure and heterogeneous cancer samples, Nat. Biotechnol. 31 (2013) 213−219.

[23] A.M. Newman, S.V. Bratman, H. Stehr, L.J. Lee, C.L. Liu, M. Diehn, A.A. Alizadeh, FACTERA: a practical method for the discovery of genomic rearrangements at breakpoint resolution, Bioinformatics (Oxford, England) 30 (2014) 3390−3393.

[24] E. Talevich, A.H. Shain, T. Botton, B.C. Bastian, CNVkit: genome-wide copy number detection and visualization from targeted DNA sequencing, PLoS Comput. Biol. 12 (2016), e1004873.

[25] K. Wang, M. Li, H. Hakonarson, ANNOVAR: functional annotation of genetic variants from high-throughput sequencing data, Nucleic Acids Res. 38 (2010) e164-e.

[26] J.-Y. Yu, S.-F. Yu, S.-H. Wang, H. Bai, J. Zhao, T.-T. An, J.-C. Duan, J. Wang, Clinical outcomes of EGFR-TKI treatment and genetic heterogeneity in lung adenocarcinoma patients with EGFR mutations on exons 19 and 21, Chin. J. Canc. (2016) 30.

[27] R. Rosell, T. Moran, C. Queralt, R. Porta, F. Cardenal, C. Camps, M. Majem, G. Lopez-Vivanco, D. Isla, M. Provencio, A. Insa, B. Massuti, J.L. Gonzalez-Larriba, et al., Screening for epidermal growth factor receptor mutations in lung cancer, N. Engl. J. Med. 361 (2009) 958−967.

[28] G. Stella, F. Rojas Llimpe, C. Barone, A. Falcone, F. Di Fabio, A. Martoni, S. Lamba, C. Ceccarelli, S. Siena, A. Bardelli, KRAS and BRAF mutational

https://doi.org/10.1016/j.heliyon.2018.e01031

status as response biomarkers to cetuximab combination therapy in advanced gastric cancer patients, J. Clin. Oncol. 27 (2009) e15503-e.

[29] N. Karachaliou, C. Mayo-de las Casas, C. Queralt, et al., Association of egfr l858r mutation in circulating free dna with survival in the eurtac trial, JAMA Oncol. 1 (2015) 149−157.

[30] S. Kobayashi, T.J. Boggon, T. Dayaram, P.A. Jänne, O. Kocher, M. Meyerson, B.E. Johnson, M.J. Eck, D.G. Tenen, B. Halmos, EGFR mutation and resistance of non−small-cell lung cancer to gefitinib, N. Engl. J. Med. 352 (2005) 786−792.

[31] N. Sueoka-Aragane, N. Katakami, M. Satouchi, S. Yokota, K. Aoe, K. Iwanaga, K. Otsuka, S. Morita, S. Kimura, S. Negoro, Hanshin-Saga Collaborative Cancer Study G, Monitoring EGFR p.T790M with plasma DNA from lung cancer patients in a prospective observational study, Cancer Sci. 107 (2016) 162−167.

[32] F. Yamaguchi, K. Fukuchi, Y. Yamazaki, H. Takayasu, S. Tazawa, H. Tateno, E. Kato, A. Wakabayashi, M. Fujimori, T. Iwasaki, M. Hayashi, Y. Tsuchiya, J. Yamashita, et al., Acquired resistance L747S mutation in an epidermal growth factor receptor-tyrosine kinase inhibitor-naïve patient: a report of three cases, Oncol. Lett. 7 (2014) 357−360.

[33] J. Bean, G.J. Riely, M. Balak, J.L. Marks, M. Ladanyi, V.A. Miller, W. Pao, Acquired resistance to epidermal growth factor receptor kinase inhibitors associated with a novel T854A mutation in a patient with EGFR-mutant lung adenocarcinoma, Clin. Canc. Res. 14 (2008) 7519−7525.

[34] Hidaka N, Iwama E, Kubo N, Harada T, Miyawaki K, Tanaka K, Okamoto I, Baba E, Akashi K, Sasaki H, Nakanishi Y. Most T790M mutations are present on the same EGFR allele as activating mutations in patients with non-small cell lung cancer. Lung Canc.. 108: 75-82.

[35] W. Pao, T.Y. Wang, G.J. Riely, V.A. Miller, Q. Pan, M. Ladanyi, M.F. Zakowski, R.T. Heelan, M.G. Kris, H.E. Varmus, KRAS mutations and primary resistance of lung adenocarcinomas to gefitinib or erlotinib, PLoS Med. 2 (2005) e17.

[36] J.A. Engelman, K. Zejnullahu, T. Mitsudomi, Y. Song, C. Hyland, J.O. Park, N. Lindeman, C.-M. Gale, X. Zhao, J. Christensen, T. Kosaka, A.J. Holmes, A.M. Rogers, et al., MET amplification leads to gefitinib resistance in lung cancer by activating ERBB3 signaling, Science 316 (2007) 1039−1043.

[37] J.A. Engelman, P.A. Jänne, Mechanisms of acquired resistance to epidermal growth factor receptor tyrosine kinase inhibitors in non−small cell lung cancer, Clin. Canc. Res. 14 (2008) 2895−2899.

https://doi.org/10.1016/j.heliyon.2018.e01031

[38] S.-F. Huang, H.-P. Liu, L.-H. Li, Y.-C. Ku, Y.-N. Fu, H.-Y. Tsai, Y.-T. Chen, Y.-F. Lin, W.-C. Chang, H.-P. Kuo, Y.-C. Wu, Y.-R. Chen, S.-F. Tsai, High frequency of epidermal growth factor receptor mutations with complex patterns in non−small cell lung cancers related to gefitinib responsiveness in Taiwan, Clin. Canc. Res. 10 (2004) 8195−8203.

[39] Z. Piotrowska, M.J. Niederst, C.A. Karlovich, H.A. Wakelee, J.W. Neal, M. Mino-Kenudson, L. Fulton, A.N. Hata, E.L. Lockerman, A. Kalsy, S. Digumarthy, A. Muzikansky, M. Raponi, et al., Heterogeneity underlies the emergence of EGFRT790 wild-type clones following treatment of T790M-positive cancers with a third-generation EGFR inhibitor, Cancer Discov. 5 (2015) 713−722.

https://doi.org/10.1016/j.heliyon.2018.e01031